

Observation, Theory, and Numerical Modeling: Atmospheric Teleconnections Leading to Generalized Frosts over Southeast South America



Gabriela V. Müller, Guillermo Berri, and Marilia de Abreu Gregorio

1 Introduction

Natural phenomena, such flooding, landslides, droughts, frosts, among others, are responsible for significant social, economic, and environmental damages and losses, which are more recurrent and have increasingly intense impacts. In particular, frosts are extreme events that directly and significantly affect human and economic activities, causing impacts and damages in various sectors. Frosts in extratropical latitudes of South America are frequent since its climate regime is characterized by incursions of air masses of polar origin, especially during the winter. They are very important in the center-northeast of Argentina, a region called Pampa Húmeda (Wet Pampa), an extended plain of more than 750,000 km². It is considered one of the world regions where the impacts are greater due to the type of production and the number of inhabitants that live there [23, 29]. In order to give proper representation to the frequent frost phenomenon that in occasions cover extended regions, [28] defined a criterion for identifying generalized frosts (GF) events, by considering the days on which a surface temperature below 0 °C is recorded at more than 75% of the meteorological stations in the Wet Pampa.

G. V. Müller (✉) · M. de A. Gregorio

Centro de Estudios de Variabilidad y Cambio Climático (CEVARCAM) – FICH – UNL, Santa Fe, Argentina

Consejo Nacional de Investigaciones Científicas y Técnicas (CONICET), Buenos Aires, Argentina

e-mail: gvmuller@fich.unl.edu.ar; mgregorio@fich.unl.edu.ar

G. Berri

Facultad de Ciencias Astronómicas y Geofísicas – UNLP, La Plata, Argentina

Consejo Nacional de Investigaciones Científicas y Técnicas (CONICET), Buenos Aires, Argentina

e-mail: gberri@fcaglp.unlp.edu.ar

© Springer Nature Switzerland AG 2019

L. Bacelar Lima Santos et al. (eds.), *Towards Mathematics, Computers and Environment: A Disasters Perspective*, https://doi.org/10.1007/978-3-030-21205-6_2

The processes that involve the development of this extremely cold condition are associated with complex interaction mechanisms in different atmospheric scales [32, 33]. Remote forcing, such as anomalous convection in the tropical region, can act as a trigger mechanism for Rossby waves generation that propagate to the extratropics, giving rise to the tropic–extratropic teleconnections [2, 12]. However, the wave propagation pattern will depend on the structure of the basic state, as well as the remote forcing [1]. The term teleconnection means remote connection and its study is a good example of the linkage between observations, theory, and numerical model results. In this work we present the linkage by means of the study of GF events in the Wet Pampa.

2 Theory of Rossby Waves

The identification of teleconnections and the analysis of their effect on the horizontal structure of the atmospheric circulation can be useful to understand the occurrence of anomalous events in various regions of the planet. It provides an overview of the atmospheric circulation in which a local forcing acts in such a way that influences remote regions. Such local forcing may be a heat source ([2, 10–12, 18, 35, 42], among others), or an orographic obstacle ([5, 7, 9, 12, 39], among others), which acts as wave generators that propagate in the atmosphere. One way to analyze the propagation of waves in the terrestrial sphere is by means of the theory of Rossby waves in a barotropic atmosphere.

2.1 Barotropic Equations

The simplest context for the study of Rossby waves is by considering a shallow layer of incompressible fluid on a rotating earth, with a simple geometry. By ignoring the effects of the earth sphericity and allowing the change with latitude of the vertical component of the earth rotation, the dynamics can be described by the two-dimensional rotating Euler equations:

$$\frac{d\mathbf{v}_H}{dt} + f\hat{k} \times \mathbf{v}_H = -\frac{1}{\rho_0}\nabla p \quad (1a)$$

$$\nabla \cdot \mathbf{v}_H = 0 \quad (1b)$$

where $\frac{d}{dt}$ is the total time derivative operator that applied to each scalar component A of the vector v_H is $\frac{d}{dt}A = \frac{d}{dt}A + (\mathbf{v} \cdot \nabla)A$, f is the Coriolis parameter, \hat{k} is the unit vertical vector, ∇p is the pressure gradient, and \mathbf{v}_H the horizontal component of the fluid flow.

Equation (1a) represents the fluid motion set by an external pressure gradient, while Eq. (1b) represents the incompressibility of the fluid. Based on the theory developed by Rossby [36, 37], the variation of the Coriolis parameter with latitude can be approximated by expanding the latitudinal dependence of f in a Taylor series about a reference latitude ϕ_0 and retaining only the first two terms to yield

$$f = f_0 + \beta y \quad (2)$$

where $\beta \equiv (df/dy)_{\phi_0} = 2\Omega \cos\phi_0/a$ and $y = 0$ at ϕ_0 . This approximation is usually referred to as the *midlatitude β -plane* approximation.

2.2 Barotropic Vorticity Equation

By imposing incompressibility, the family of sound waves is removed from the set of possible solutions, yet the Coriolis parameter provides a restoring mechanism leading to the nontrivial, the so-called Rossby wave solution. To promptly set equations for describing the Rossby waves, the non-divergence condition $\nabla \cdot \mathbf{v}_H = 0$ allows us to describe the problem in stream-function formulation ψ , with $\mathbf{v}_H = \hat{k} \times \nabla\psi$.

Thus, taking the curl of Eq. (1a), the non-linear, the non-divergent barotropic Rossby waves are described by Charney [6], Pedlosky [34] as:

$$\frac{\partial \zeta}{\partial t} + J(\psi, \zeta) + \beta \frac{\partial \psi}{\partial x} = 0 \quad (3)$$

where $\zeta = \nabla^2\psi = \hat{k} \cdot (\nabla \times \mathbf{v}_H)$, and β is the meridional derivative of the Coriolis parameter.

The non-linear contribution in Eq. (3) is clearly due to the Jacobian

$$J(\psi, \zeta) = \left[\frac{\partial \psi}{\partial x} \frac{\partial \zeta}{\partial y} - \frac{\partial \psi}{\partial y} \frac{\partial \zeta}{\partial x} \right] \quad (4)$$

which represents the advection of the relative vorticity ζ since $\mathbf{v}_H = \hat{k} \times \nabla\psi$.

When the advective contribution is linearized by approximating $J(\psi, \zeta) \approx \bar{U}(y) \frac{\partial}{\partial x} \zeta$ with a time invariable westerly flow with meridional shear $\bar{U}(y)$, we obtain the following wave equation:

$$\frac{\partial \zeta}{\partial t} + \bar{U}(y) \frac{\partial \zeta}{\partial x} + \beta \frac{\partial \psi}{\partial x} = 0 \quad (5)$$

Equation (5) is in terms of the stream function ψ that can be expressed as:

$$\psi' = \psi_0 e^{i(kx+ly-\sigma t)} \quad (6)$$

so that the relative vorticity results in terms of the perturbation stream function as $\zeta' = \nabla^2 \psi'$ (since $\zeta_0 = 0$). Thus the solution allows to obtain the following frequency:

$$\sigma = k\bar{U} - \frac{\beta^+ k}{k^2 + l^2} \quad (7)$$

where the generalized β^+ parameter, the meridional gradient of absolute vorticity, is given by:

$$\beta^+ = \beta - \frac{\partial^2 \bar{U}}{\partial y^2} \quad (8)$$

On the other hand, the wave activity in the plane propagates with the group velocity whose components are obtained by deriving the frequency with respect to the wave numbers k and l :

$$c_g = (u_g, v_g) = (\partial\sigma/\partial k, \partial\sigma/\partial l) = (c, 0) + \left(\frac{2\beta^+}{K^2}\right) \cos(\alpha) \hat{K} \quad (9)$$

where $c = \sigma/k$ is the eastward phase velocity, \hat{K} is the unit vector normal to the trough and ridge axis with an eastward positive component, and α is the angle the vector forms with the eastward direction. In addition, the total stationary Rossby wave number K_s is obtained by making $\sigma = 0$ in Eq. (7):

$$K_s = \sqrt{\frac{\beta^+}{\bar{U}}} \quad (10)$$

Therefore, the development of stationary Rossby waves is possible only in a westerly flow ($\bar{U} > 0$) as long as β^+ is always positive. From Eqs. (9) and (10), the group velocity for stationarity condition:

$$\mathbf{c}_{gs} = 2\bar{U} \cos \alpha \hat{K} \quad (11)$$

Thus for the stationary Rossby waves, the energy propagates perpendicular to the axis of the ridges and troughs with velocity equal to $2\bar{U} \cos \alpha$. In sum, this theory describes how an initial vorticity source in a barotropic atmosphere with a stationary zonal flow is able to generate a series of ridges and troughs whose energy is dispersed with a group velocity given by Eq. (11). The resulting wave trains are linked to the observed teleconnection patterns ([12, 16], among others). In particular, the Southern Hemisphere offers a unique environment to test the propagation of these waves in observed atmospheric circulation patterns, due to the equivalent

barotropic structure of the atmosphere and the prevalent zonal structure of the time mean flow [19]. According to [17] a useful diagnostic tool for representing the mean background state in which the transients are embedded is the calculation of K_s given by Eq. (10) which is the total wave number at which a barotropic Rossby wave is stationary at a particular location and in a given background zonal flow (\bar{U}).

3 Local Forcings of Rossby Waves

Rossby waves are a type of atmospheric motion due to the conservation of absolute vorticity and the variation of the Coriolis parameter with latitude, the so-called β -effect. This synoptic scale wave motion in the horizontal plane is characterized by the alternation of regions of cyclonic and anticyclonic vorticity as the wave propagates, and the restoring force of this wave is the Coriolis force. One of the factors favoring Rossby waves generation is tropical diabatic heating, which is balanced by vertical upward motion and upper-level divergence resulting in a disturbance of the relative vorticity field. Hoskins et al. [12] used a barotropic model to study the atmospheric response to a thermal forcing and found the influence of tropical heating and upper-level divergence on the generation of Rossby waves that propagate along extratropical curved pathways in the form of wave trains associated with teleconnections. The forcing for the Rossby waves in a divergent field can be inferred by means of the barotropic vorticity equation:

$$\frac{\partial \xi}{\partial t} + \mathbf{v} \cdot \nabla \xi = -\xi D \quad (12)$$

where $\xi = f + \zeta$ is the absolute vorticity, f the planetary vorticity, ζ the relative vorticity, \mathbf{v} the wind vector, and $D = \partial u/\partial x + \partial v/\partial y$ is the horizontal divergence. The left-hand side of the equation describes the Rossby wave propagation, while the right-hand side represents the forcing. However, as ξ is relatively small in the tropics, the heating anomalies in the tropics would be ineffective to produce Rossby waves, which does not match the observed teleconnection patterns. In order to analyze in more detail the barotropic vorticity equation, the wind vector can be expressed as the sum of a rotational (v_ψ) and a divergent (v_χ) component, in terms of a stream function ψ and a velocity potential χ , respectively, as follows:

$$v_\psi = k \times \nabla \psi \quad (13)$$

$$v_\chi = \nabla \chi \quad (14)$$

Therefore, the relative vorticity can be written as $\zeta = \nabla^2 \psi$ and the divergence as $D = \nabla^2 \chi$. By replacing \mathbf{v} as $v_\psi + v_\chi$, the barotropic vorticity equation becomes:

$$\frac{\partial \xi}{\partial t} + v_\psi \cdot \nabla \xi = -\xi D - v_\chi \cdot \nabla \xi \quad (15)$$

In this way, the left-hand side of the equation involves the rotational part and the right-hand side the divergent part of the wind. Sardeshmukh and Hoskins[38] discussed this equation and identified the right-hand side terms as Rossby waves sources by the divergent wind, S , as follows:

$$S = -\xi D - v_\chi \cdot \nabla \xi \quad (16)$$

Thus, the forcing for Rossby waves will be greater in areas where the divergence, the divergent wind, the absolute vorticity, or its gradient is larger. This may take place in the Southern Hemisphere regions southward of the equator where the upper-level divergence associated with deep convection is larger and there are large vorticity gradients associated with the subtropical jet. The previous equation indicates that Rossby waves can be excited by tropical diabatic heating even though ξ may be small in regions where the heating takes place, since the divergent flow will be larger there. Towards the subtropics the gradient of ξ is larger, contributing to higher values of S . We can rewrite the previous equation as:

$$S = S1 + S2 \quad (17)$$

where $S1 = -\xi D$ is the term of vortex stretching that represents the generation of vorticity by divergence and $S2 = -v_\chi \cdot \nabla \xi$ is the advection of absolute vorticity by the divergent flow. Lu and Kim[20] used these expressions to evaluate the role of tropical and extratropical heating in the generation of Rossby waves in the Northern Hemisphere. Sardeshmukh and Hoskins[38] highlighted the importance of the advection term of absolute vorticity by the divergent flow in their study of the atmospheric response to tropical divergence over the western Pacific Ocean. The local forcings are applied in the experiments described in Sect. 6 using the model presented in the following section.

4 Model IGCM

The baroclinic model IGCM (Intermediate Global Circulation Model—Center for Global Atmospheric Modeling, University of Reading) was used in several studies, like [2, 5, 15, 21]. Although the model is dry and does not include any physical process linked to the phase change of water vapor, many aspects of the atmospheric dynamics can be reproduced, from synoptic scale systems [13] to large-scale perturbations [43]. IGCM is a baroclinic model that runs on a global domain, with a T42 spectral truncation of the zonal wave number, and includes horizontal and vertical diffusion and Newtonian cooling [15]. The large-scale dynamics of the atmosphere can be interpreted in qualitative terms by means of the linear theory of waves because there is a good agreement between IGCM results and those obtained with the barotropic [2].

The model is global and is formulated on a sphere with a multi-level vertical coordinate. In the horizontal, it uses a spectral representation and in the vertical a finite difference scheme with a semi-implicit method in which the terms of linearized gravity waves are time averages so that the faster movements are smoothed for the time integration. Blackburn [3] included an alternative vertical scheme based on that used by the ECMWF [41] that preserves the angular momentum since the original finite difference scheme did not.

The horizontal equations of motion are expressed in the form of vorticity and divergence, which is convenient when using spectral techniques and semi-implicit time schemes. The equations of motion are formulated in dimensionless form, on a rotating sphere, assuming a hydrostatic and adiabatic perfect gas, without viscosity:

$$\frac{\partial \xi}{\partial t} = \frac{1}{1 - \mu^2} \frac{\partial \mathcal{J}_v}{\partial \lambda} - \frac{\partial \mathcal{J}_u}{\partial \mu} \quad (18)$$

$$\frac{\partial D}{\partial t} = \frac{1}{1 - \mu^2} \frac{\partial \mathcal{J}_v}{\partial \lambda} - \frac{\partial \mathcal{J}_u}{\partial \mu} - \nabla^2 \left(\frac{U^2 + V^2}{2(1 - \mu^2)} + \phi + \bar{T} \ln p_* \right) \quad (19)$$

$$\frac{\partial T'}{\partial t} = \frac{-1}{1 - \mu^2} \frac{\partial}{\partial \lambda} (UT') - \frac{\partial}{\partial \mu} (VT') + DT' - \dot{\sigma} \frac{\partial T}{\partial \sigma} + k \frac{T\omega}{p} \quad (20)$$

$$\frac{\partial \ln p_*}{\partial t} = -V \cdot \nabla \ln p_* - D - \frac{\partial \dot{\sigma}}{\partial \sigma} \quad (21)$$

$$\frac{\partial \phi}{\partial \ln \sigma} = -T \quad (22)$$

With \mathcal{J}_u and \mathcal{J}_v defined as follows:

$$\mathcal{J}_u = V\xi - \dot{\sigma} \frac{\partial U}{\partial \sigma} - T' \frac{\partial \ln p_*}{\partial \lambda} \quad (23)$$

$$\mathcal{J}_v = U\xi - \dot{\sigma} \frac{\partial V}{\partial \sigma} - T'(1 - \mu^2) \frac{\partial \ln p_*}{\partial \lambda} \quad (24)$$

where ξ is the absolute vorticity, D the divergence, $T = T(\sigma) + T'$ the temperature, p_* the surface pressure, ϕ the geopotential, σ is the vertical coordinate pressure, ω is the vertical velocity, λ is the longitude, and $\mu = \sin\theta$, where θ is the latitude. The horizontal advection operator is

$$V \cdot \nabla = \frac{U}{1 - \mu^2} \left(\frac{\partial}{\partial \lambda} \right) + V \left(\frac{\partial}{\partial \mu} \right) \quad (25)$$

The velocity potential χ and the stream function ψ are introduced in this form:

$$U = - \left(1 - \mu^2 \right) \frac{\partial \psi}{\partial \mu} + \frac{\partial \chi}{\partial \lambda} \quad (26)$$

$$V = \frac{\partial \psi}{\partial \lambda} + (1 - \mu^2) \frac{\partial \chi}{\partial \mu} \quad (27)$$

$$\xi = 2\mu + \frac{1}{1 - \mu^2} \frac{\partial V}{\partial \lambda} - \frac{\partial U}{\partial \mu} = 2\mu + \nabla^2 \psi \quad (28)$$

$$D = \frac{1}{1 - \mu^2} \frac{\partial U}{\partial \lambda} + \frac{\partial V}{\partial \mu} = \nabla^2 \chi \quad (29)$$

The vorticity ξ , the divergence D , and the temperature T at each level, as well as the logarithm of the surface pressure p_* , are expressed as a series of the form:

$$A = \sum_{m=-M}^M \sum_{n=|m|}^N A_n^m Y_n^m(\mu, \lambda) \quad (30)$$

where A represents any of those variables and λ is the longitude, μ the sine of the latitude, A_n^m is a complex coefficient, $Y_n^m = P_n^m(\mu)e^{im\lambda}$ is a spherical harmonic, where P_n^m a standard Legendre function, m is the zonal wave number, $n - m$ is the number of zeros between the north and south poles, n is the total wave number, and N, M are the truncation wave numbers defined as the largest number of wave retained in the spectral series.

The model employs jagged triangular truncation of the total wave number 42, which allows an independent representation of the position in the sphere. It can be executed in a wide range of horizontal and vertical resolutions. It has 12 vertical equally spaced levels which are chosen so that the resolution everywhere is lower than 105 hPa, with higher resolution near the tropopause. The model equations are integrated using a spectral transformation method as described in detail by Bourke [4].

Equation (18) is expressed in spherical coordinates, but the conservation of absolute vorticity $\xi = \zeta + f$ can be written in Cartesian coordinates as:

$$\frac{d\xi}{dt} = -V \cdot \nabla \xi \quad (31)$$

So that:

$$\frac{\partial \zeta}{\partial t} = u \frac{\partial}{\partial x} (\zeta + f) + v \frac{\partial}{\partial y} (\zeta + f) \quad (32)$$

$$= u \frac{\partial}{\partial x} (\zeta + f) + v \frac{\partial \zeta}{\partial y} + v \frac{\partial f}{\partial y} \quad (33)$$

Replacing in Eq. (31), $\frac{\partial f}{\partial y} = \beta$, $u = -\frac{\partial \psi}{\partial y}$, $v = \frac{\partial \psi}{\partial x}$, we obtain Eq. (3).

5 Preferential Paths of Rossby Waves Propagation

The wave theory provides a simple and useful interpretation of global Rossby wave propagation. This theory describes how an initial vorticity source in a barotropic atmosphere with a stationary zonal flow (Eq. (5)) is able to generate a series of ridges and troughs whose energy is dispersed with a group velocity given by (Eq. (11)). The resulting wave trains are linked to the observed teleconnection patterns ([12, 16], among others). In particular, the Southern Hemisphere offers a unique environment to test the propagation of these waves in observed atmospheric patterns, due to the equivalent barotropic structure of the atmosphere and the prevalent zonal structure of the time mean flow [19]. The following questions arise, which are the preferential paths of wave propagation, and where are the waves originated?

A useful diagnostic tool for representing the mean background state in which the transients are embedded is the calculation of K_s given by Eq. (10) which is the total wave number at which a barotropic Rossby wave is stationary at a particular location and in a given background zonal flow (\bar{U}) [17]. According to this theory, the characteristics of the Rossby wave propagation in a given basic state may be determined by the analysis of K_s . Hoskins and Ambrizzi [11], among others, showed that the distribution of K_s can be used to infer the location of critical lines and waveguides for stationary Rossby waves. For example, zonally oriented regions of relative high values of K_s bounded by lower values to the north and south (usually associated with strong jet streams) indicate favorable locations for guiding Rossby waves.

Based on the large-scale physical mechanisms associated with GF, manifested through teleconnection patterns given by stationary Rossby waves, [24] used K_s to give a qualitative picture of the effects of the basic state flow within the westerly duct on the subtropical and polar wave propagation. This was a first assessment of the impact of the GF basic flow on the dynamical structure relevant for the Rossby wave dispersion. Using this theoretical concept, the distribution of the stationary wave number (K_s) in the Southern Hemisphere is obtained for the two opposite basic states given by the composition of winters with maximum and minimum frequency of GF occurrence in the Wet Pampa. To understand the large-scale atmospheric circulation associated with these cold episodes, [30] identified years of extreme frequency of frost occurrence, during the period 1961–1990. A maximum (minimum) frequency of GF occurrence is considered when the number of frosts is one standard deviation (σ) above (below) the mean value during the austral winter (JJA), i.e., GF $+\sigma$ and GF $-\sigma$, respectively.

From these fields it is possible to determine preferential wave propagation paths that reach South America. The distribution of K_s emphasizes the importance of the jets as efficient waveguides, with a good agreement between their positions and the bands of local K_s maxima, with zonal orientation. Nevertheless, there are differences between both analyzed basic states, which explain in part why there are winters with GF $+\sigma$ and GF $-\sigma$, as shown by Müller and Ambrizzi [24]. The geographic distribution of K_s is shown in Fig. 1a, b with the zero wind contours,

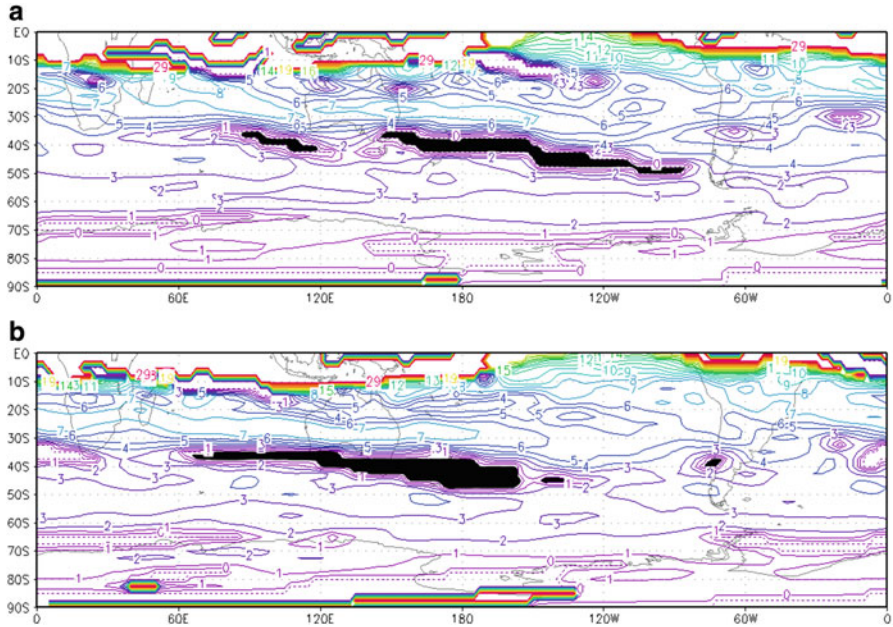


Fig. 1 Stationary wave number K_s at 250 hPa, corresponding to (a) GF $+\sigma$ and (b) GF $-\sigma$ (from [24])

$\bar{U} = 0$, in thick color lines, while those corresponding to zero K_s (i.e., $\beta^+ = 0$) in dotted lines. The equatorial belt is dominated by a sector where the propagation is inhibited due to the presence of a transition from westerly to easterly flow, which forms a “critical line” for the propagation of stationary Rossby waves. This region is marked with thicker lines in Fig. 1a, b indicating high wave number values ($K_s \geq 20$).

A local maximum of K_s in the region of maximum zonal winds, i.e., along the subtropical jet (see Fig. 2a, b), shows wave numbers 6 and 7 in both winter groups. This region also contains uniform values of K_s meridionally limited by smaller ones. In the polar side of the subtropical jet the presence of $K_s = 0$ (the black shaded region) inhibits the propagation of Rossby waves through it because, according to the wave theory, they must deviate before reaching this region, so that the $K_s = 0$ line acts as a waveguide boundary. An interesting feature of this last case is the difference in the longitudinal extension of K_s for GF $+\sigma$ with respect to GF $-\sigma$. In Fig. 1a this region extends very near to the South American continent. However, the K_s pattern for the GF $-\sigma$ winters (Fig. 1b) shows a shorter extension of the waveguide duct, besides of a region of zero K_s between 35°S and 40°S in the west of Argentina, which coincides with the main entrance region of weather systems over South America ([8, 40], among others). This feature is not seen in the GF $+\sigma$ winters and it may have some influence on the Rossby waves propagation paths and, therefore, in the frost events.

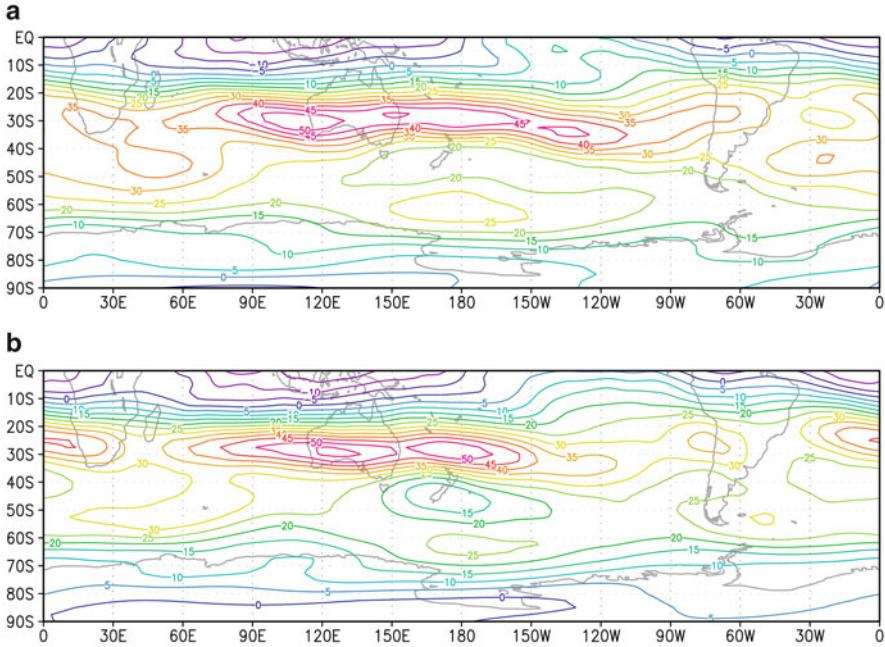


Fig. 2 Mean zonal wind component (ms^{-1}) at 250 hPa for the austral winters, corresponding to (a) $\text{GF} +\sigma$ and (b) $\text{GF} -\sigma$ (from [24])

Another characteristic of both basic states can be seen in Fig. 2a, b that shows regions of maximum mean zonal wind of winters with $\text{GF} +\sigma$ and $\text{GF} -\sigma$. The main basic state feature for $\text{GF} +\sigma$ winters (Fig. 2a) shows maximum values of mean zonal 250 hPa wind around 30°S extending from the Indian Ocean to the Pacific Ocean. The core maximum is around 50 ms^{-1} and is located over the eastern Indian Ocean, being displaced 60° to the west of the climatological reference mean (winter JJA 1961–1990). The 35 ms^{-1} contour reaches the South American continent with a second nucleus extending southeastward from southern South Africa. An outstanding characteristic is the magnitude of zonal wind gradient over the southwestern Indian Ocean. The zonal wind maxima at high latitudes, between 20 and 25 ms^{-1} , are located along the 60°S and the polar jet position is also different from that of the climatology with a “tongue” towards South America with a longitudinal extension that brings it closer to the continent [24]. In the case of $\text{GF} -\sigma$ winters (Fig. 2b) the subtropical jet is divided in two zones, one from the Atlantic Ocean up to South Africa and other from the Indian Ocean up to the central Pacific Ocean. In this last case, the subtropical jet has two maxima around 30°S , one to the southwest of Australia and the other one at approximately the dateline with a secondary maximum to the south of it.

However, the propagation of Rossby waves depends not only on the basic state in which they are, but also on the generating source of these waves [1]. In this

sense, [23, 24, 31] performed numerical experiments with the multi-level baroclinic general circulation model IGCM, which is an appropriate tool to study the physical mechanisms of wave propagation since the response can be directly attributed to the generating source.

6 Source Regions of Rossby Waves

In order to test the generation of extratropical wave patterns which favor the development of extreme cold events over the southeast of South America, numerical simulations using IGCM were carried out. Müller [23, 24, 31] simulated with the IGCM the Rossby wave pattern responsible for the teleconnection, with two basic states given by the composition of winters with GF $+\sigma$ and GF $-\sigma$ in the Wet Pampa.

The model IGCM is run in two steps according to [23, 24, 31]. The first one consists of the buildup of the initial basic state, with which the model reaches the steady state, using geopotential heights, zonal and meridional wind, and temperature at 12 vertical sigma levels. The second step consists of the perturbation of the model by introducing a thermal forcing. The heating source has an elliptical horizontal structure and a fixed position in latitude and longitude. The vertical heating profile follows a cosine function with the maximum amplitude at 400 hPa corresponding to a $5^\circ\text{C}/\text{day}$ and decaying to zero at the surface and the top of the model. This value is equivalent to a latent heat release associated with 10 mm of precipitation. Although one may question the realism of this heating source, its role here is purely of acting as a Rossby wavemaker [24, 31]. The combination of observed tropical convection and a specific basic state can create the appropriate environment to guide Rossby waves triggered by the tropical forcing towards South America [31]. In particular, stationary Rossby waves may be one important mechanism linking anomalous tropical convection with the extreme cold events in the Wet Pampas [31]. The theory of Rossby wave propagation supports the obtained result by means of ray tracing computation (derived from Eq. (10)), by placing the forcing in the position of the anomalous tropical convection [25], so that they act as a thermal forcing proxy for the model. The areas of anomalous convection and, consequently, the position of the heat source, are identified with the observed outgoing longwave radiation (OLR) compositions of the extreme GF $+\sigma$ and GF $-\sigma$ winters. [31] found, during GF $+\sigma$ winters, two main regions of anomalous tropical convection in the Southern Hemisphere located over the Indian and the western Pacific Oceans, respectively, with significant values. On the other hand, during GF $-\sigma$ winters there were no significant OLR regions that could act as sources of Rossby waves [31].

Numerical simulations with the IGCM model were performed by Müller et al. [31], considering the position of the forcing according to the observations in both basic states. The result of the experiment with the GF $+\sigma$ basic state and the heat source located over the western Pacific Ocean shows a pattern of wind anomalies with an arc-shaped trajectory of Rossby waves, which initially goes to the South

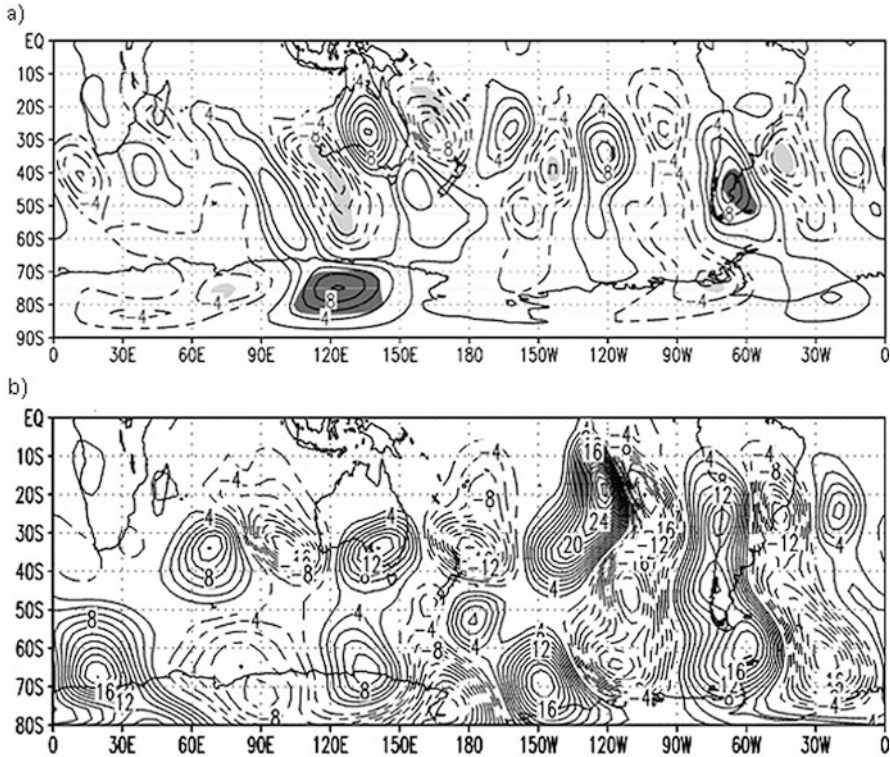


Fig. 3 (a) Composites of observed meridional wind field anomalies at 250 hPa for GF + σ . Positive (negative) contours are in solid (dotted) lines at 1.5 ms⁻¹ intervals (from [30]). (b) Meridional wind component anomalies (ms⁻¹) at 250 hPa for day 14 of integration, corresponding to the simulation of GF + σ basic state (from [24])

Pole and then turns towards the equator. This wave train reaches South America in its central part and creates southerly wind anomalies across the southern tip of the continent. However, when analyzing the experiment with the basic state GF - σ , the obtained pattern does not correspond to the preferred paths that the waves follow during the winter in the Southern Hemisphere. In this case it is possible to observe two waves trains that bifurcate from their region of origin [31].

Depending on the phase with which the waves enter the South American continent, they can favor the southerly cold and dry air advection by anomalous winds at low levels, over the whole southern extreme of the continent, leading to frosts occurrence in the Wet Pampa region [31]. However, the pattern obtained with the numerical experiments and the forcings located over the Indian Ocean and the western Pacific Oceans, respectively, are not able to explain the observed anomalies in the mass and wind fields as reported by Müller et al. [30]. These authors have shown that for GF + σ winters, the synoptic scale waves spread over the South Pacific Ocean along the subpolar and the subtropical jets (Fig. 3a).

This behavior is clearly observed during the days previous to the event. When the waves are closer to the Andes Mountains they extend meridionally and form an NW–SE oriented arc, shifting progressively towards the NE leeward to the Andes. Once the waves have crossed the Andes Mountains, they spread towards the North in such a way that is consistent with the concept of Rossby wave dispersion on a sphere [14].

In order to obtain the results observed in [30], new numerical IGCN experiments were designed that allowed further understanding of the role played by the remote forcing as source of Rossby waves finally responsible for the GF events. Müller and Ambrizzi [24] performed new simulations with the same two basic states of GF $+\sigma$ and GF $-\sigma$, considering the regions where the propagation of these waves is favored by K_s and where the zonal wind maxima are, i.e., the jets location. In a particular numerical simulations performed for GF $+\sigma$ (Fig. 3b), the patterns are consistent with the observed ones (Fig. 3a). From the results obtained by Müller and Ambrizzi [24], a conceptual model is proposed which arises from the observations, the theory, and the numerical modeling.

7 Conceptual Model

In a basic state that favors the occurrence of GF $+\sigma$, Rossby waves are generated over the tropical Indian Ocean in a mean flow characterized by a meridional gradient of zonal wind (indicated with arrows in Fig. 4). The upper-level divergent motion (dashed arrow), probably generated by a tropical source (red circle), generates perturbations in the subtropics by interfering with the positive meridional gradient of absolute vorticity region that will finally become the source of Rossby waves. This source region is upstream of the Australian subtropical jet and upstream the region where the meridional gradient of absolute vorticity is negative (stripped area). According to the linear wave theory, this region will reflect the waves, not allowing their propagation through it, so that waveguide ducts are created to the north and the south of the region. In this way, the generated Rossby waves (represented by the sequence of positive—full lines—and negative—dashed lines—meridional wind anomaly regions) propagate along the subtropical and polar waveguides (thick arrows). Near the South American continent the phases of both wave trains coincide over the region where the propagation inhibition disappears, merging into one single pattern. The deep ridge over the western part of the continent produces strong cold air advection by southerly winds (thick arrows), extending through the whole troposphere, before the occurrence of a GF event. Hence, the cold air starts crossing the Andes mountain range, initially where the heights are lower, i.e., in southern South America, generating anticyclonic vorticity. The advection of anticyclonic vorticity feeds the continental anticyclone and the maritime cyclone situated downstream over the Atlantic Ocean. The increase of the pressure gradient over the area creates a strong southerly wind component between the high and

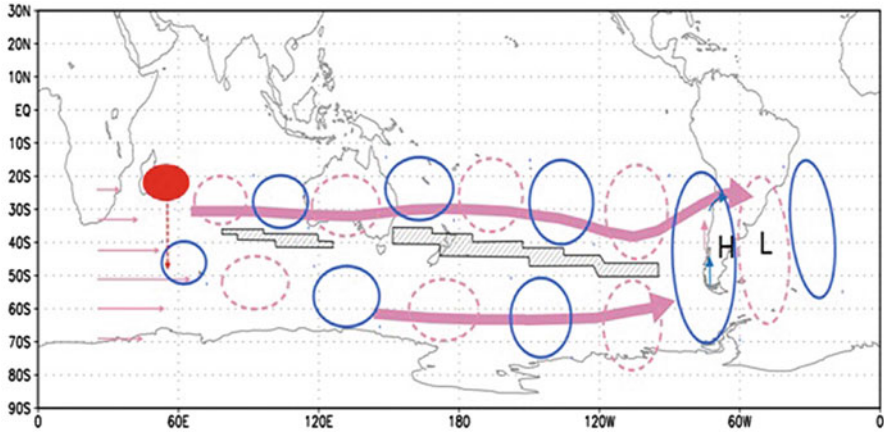


Fig. 4 Conceptual model of the physical mechanisms that favor a maximum frequency of GF occurrence during austral winters and the more persistent GF events. The Rossby wave train of meridional wind anomalies in solid (dashed) lines represents positive (negative) values. The combination of colors means that the results were obtained by: observations (pink), theory (black), and model (blue). The H and L symbols indicate the position of the low level anticyclone and cyclone, respectively. See text for details (from [24])

low pressure systems, bringing cold polar air to the region which finally leads to a significant drop of surface temperature over the eastern part of the continent.

The above described mechanism is also valid for explaining the conditions of the GF persistence as shown by Müller and Berri [26, 27] who grouped them based on the number of consecutive days during which the frost conditions persisted in the region. The persistence of the GF phenomenon depends on whether there is one or two wave trains approaching the South American continent and, in the last case, on how they merge. However, the former is not the only element that will define the GF persistence. It is at this point that linearity is diluted in the chaotic nature of any physical system and its mathematical treatment must take into account non-linear solutions such as the advection of cold air coming from the south in a sustained way, for a certain period of time, and at different levels of the atmosphere. In addition, there are other intervening factors in different scales of the atmospheric motion that should be taken into account such as the influence of the mountain range, the subsidence of the northerly flow resulting from a transverse circulation to the jet, and the confluence (diffluence) of the flow in the entry (exit) region of the subtropical jet ([26, 27], among others).

8 Conclusions

Extreme cold events have a strong impact in central-southern South America due to their spatial extension, and they are especially important when they become persistent and frequent. The impact of generalized frosts (GF) in midlatitude regions such as the Wet Pampa is more related to frost frequency and persistence with which they occur than to its intensity, in particular when they take place during cold and prolonged winters [27]. The atmospheric circulation features associated with the frequency of frosts occurrence in the Wet Pampa region have been explored [22–25, 30, 31] and, on the other hand, the dynamic conditions that favor the persistence of these events were studied by Müller and Berri [26, 27]. The results of these studies were obtained by relating observations, linear theory, and modeling, so it was possible to formulate a conceptual scheme (Fig. 4) to explain the teleconnection mechanisms that act in particular during the austral winters of maximum frequency of GF occurrence, in coincidence with those that explain the more persistent events. In this case, other scales of atmospheric motion intervene with the large scale that finally define the persistence of the GF event. Since the interaction between different scales of motion is mainly responsible for the energy exchanges in the atmosphere, new analyses were performed [32, 33], although it is necessary to profound the studies in order to further the understanding of non-linear GF phenomena.

References

1. Ambrizzi, T., Hoskins, B.J., Hsu, H.H.: Rossby wave propagation and teleconnection patterns in the austral winter. *J. Atmos. Sci.* **52**(21), 3661–3672 (1995)
2. Ambrizzi, T., Hoskins, B.J.: Stationary Rossby-wave propagation in a baroclinic atmosphere. *Q. J. R. Meteorol. Soc.* **123**, 919–928 (1997)
3. Blackburn M.: Program description for the multi-level global spectral model. Dept. of Meteorology, University of Reading (1985)
4. Bourke W.: A multi-level spectral model I: formulation and hemispheric integrations. *Mon. Weather Rev.* **102**, 678–701 (1974)
5. Cavalcanti, I.F.: Teleconnection patterns orographically induced in model results and from observational data in the austral winter of the Southern Hemisphere. *Int. J. Climatol.* **20**(10), 1191–1206 (2000)
6. Charney, J.G.: On the scale of atmospheric motions. *Geophys. Publ. Oslo* **17**, 1–17 (1948)
7. Gan, M.A., Rao, V.B.: The influence of the Andes Cordillera on transient disturbances. *Mon. Weather Rev.* **122**(6), 1141–1157 (1994)
8. Garreaud, R.: Cold air incursions over subtropical South America: mean structure and dynamics. *Mon. Weather Rev.* **128**(7), 2544–2559 (2000)
9. Grose, W.L., Hoskins, B.J.: On the influence of orography on large-scale atmospheric flow. *J. Atmos. Sci.* **36**(2), 223–234 (1979)
10. Horel, J.D., Wallace, J.M.: Planetary-scale atmospheric phenomena associated with the Southern Oscillation. *Mon. Weather Rev.* **109**(4), 813–829 (1981)
11. Hoskins, B.J., Ambrizzi, T.: Rossby wave propagation on a realistic longitudinally varying flow. *J. Atmos. Sci.* **50**(12), 1661–1671 (1993)

12. Hoskins, B.J., Karoly, D.J.: The steady linear response of a spherical atmosphere to thermal and orographic forcing. *J. Atmos. Sci.* **38**(6), 1179–1196 (1981)
13. Hoskins, B.J., Simmons, A.J.: A multi-layer spectral model and the semi-implicit method. *Q. J. R. Meteorol. Soc.* **101**(429), 637–655 (1975)
14. Hsu, H. H.: Propagation of low-level circulation features in the vicinity of mountain ranges. *Mon. Weather Rev.* **115**(9), 1864–1893 (1987)
15. Jin, F., Hoskins, B.J.: The direct response to tropical heating in a baroclinic atmosphere. *J. Atmos. Sci.* **52**(3), 307–319 (1995)
16. Karoly, D.J.: Rossby wave propagation in a barotropic atmosphere. *Dyn. Atmos. Oceans* **7**(2), 111–125 (1983)
17. Kiladis, G.N.: Observations of Rossby waves linked to convection over the eastern tropical Pacific. *J. Atmos. Sci.* **55**(3), 321–339 (1998)
18. Li, L., Nathan, T.R.: The global atmospheric response to low-frequency tropical forcing: zonally averaged basic states. *J. Atmos. Sci.* **51**(23), 3412–3426 (1994)
19. Loon, H., Jenne, R.L.: The zonal harmonic standing waves in the Southern Hemisphere. *J. Geophys. Res.* **77**(6), 992–1003 (1972)
20. Lu, R., Kim, B.J.: The climatological Rossby waves source over the STCZs in the Summer Northern Hemisphere. *J. Meteorol. Soc. Jpn.* **82**(2), 657–669 (2004)
21. Marengo, J.A., Ambrizzi, T., Kiladis, G., Liebmann, B.: Upper-air wave trains over the Pacific Ocean and wintertime cold surges in tropical-subtropical South America leading to Freezes in Southern and Southeastern Brazil. *Theor. Appl. Climatol.* **73**(3–4), 223–242 (2002)
22. Müller, G.V.: Patterns leading to extreme events in Argentina: partial and generalized frosts. *Int. J. Climatol.* **27**(10), 1373–1387 (2007)
23. Müller, G.V.: Temperature decrease in the extratropics of South America in response to a tropical forcing during the austral winter. *Ann. Geophys.* **28**(1), 1 (2010)
24. Müller, G.V., Ambrizzi, T.: Teleconnection patterns and Rossby wave propagation associated to generalized frosts over southern South America. *Clim. Dyn.* **29**(6), 633–645 (2007)
25. Müller, G.V., Ambrizzi, T.: Rossby wave propagation tracks in southern hemisphere mean basic flows associated to generalized frosts over southern South America. *Atmósfera* **23**(1), 25–35 (2010)
26. Müller, G.V., Berri, G.J.: Atmospheric circulation associated with persistent generalized frosts in central-southern South America. *Mon. Weather Rev.* **135**(4), 1268–1289 (2007)
27. Müller, G.V., Berri, G.J.: Atmospheric circulation associated with extreme generalized frosts persistence in central-southern South America. *Clim. Dyn.* **38**(5–6), 837–857 (2012)
28. Müller, G.V., Nuñez, M.N., Seluchi, M.E.: Relationship between ENSO cycles and frost events within the Pampa Humeda region. *Int. J. Climatol.* **20**(13), 1619–1637 (2000)
29. Müller, G.V., Compagnucci, R., Nuñez, M., Salles, A.: Surface circulation associated with frosts in the wet Pampas. *Int. J. Climatol.* **23**(8), 943–961 (2003)
30. Müller, G.V., Ambrizzi, T., Nuñez, M.N.: Mean atmospheric circulation leading to generalized frosts in central southern South America. *Theor. Appl. Climatol.* **82**(1–2), 95–112 (2005)
31. Müller, G.V., Ambrizzi, T., Ferraz, S.E.: The role of the observed tropical convection in the generation of frost events in the southern cone of South America. *Ann. Geophys.* **26**(6), 1379–1390 (2008)
32. Müller, G.V., Gan, M.A., Dal Piva, E., Silveira, V.P.: Energetics of wave propagation leading to cold event in tropical latitudes of South America. *Clim. Dyn.* **45**(1–2), 1–20 (2015)
33. Müller, G.V., Gan, M.A., Dal Piva, E.: Energetics of wave propagation leading to frost events in South America: extratropical latitudes. *Atmos. Sci. Lett.* **18**(8), 342–348 (2017)
34. Pedlosky, J.: *Geophysical Fluid Dynamics*. Springer, Berlin (1987)
35. Rasmusson, E.M., Mo, K.: Linkages between 200-mb tropical and extratropical circulation anomalies during the 1986–1989 ENSO cycle. *J. Clim.* **6**(4), 595–616 (1993)
36. Rossby, C.G.: Relation between variations in the intensity of the zonal circulation of the atmosphere and the displacements of the semi-permanent centers of action. *J. Mar. Res.* **2**, 38–55 (1939)

37. Rossby, C.G.: On the propagation of frequencies and energy in certain types of oceanic and atmospheric waves. *J. Meteorol.* **2**(4), 187–204 (1945)
38. Sardeshmukh, P.D., Hoskins, B.J. The generation of global rotational flow by steady idealized tropical divergence. *J. Atmos. Sci.* **45**(7), 1228–1251 (1988)
39. Satyamurty, P., Dos Santos, R.P., Lems, M.A.M.: On the stationary trough generated by the Andes. *Mon. Weather Rev.* **108**(4), 510–520 (1980)
40. Seluchi M.E., Marengo J.A.: Tropical-midlatitude exchange of air masses during summer and winter in South America: climatic aspects and examples of intense events. *Int. J. Climatol.* **20**, 1167–1190 (2000)
41. Simmons A.J., Burridge D.M.: An energy and angular-momentum conserving vertical finite-difference scheme and hybrid vertical coordinates. *Mon. Weather Rev.* **109**, 758–766 (1981)
42. Tyrrell, G.C., Karoly, D.J., McBride, J.L.: Links between tropical convection and variations of the extratropical circulation during TOGA COARE. *J. Atmos. Sci.* **53**(18), 2735–2748 (1996)
43. Valdes, P.J., Hoskins, B.J.: Linear stationary wave simulations of the time-mean climatological flow. *J. Atmos. Sci.* **46**(16), 2509–2527 (1989)